Development of an Incremental Model for Fatigue Crack Growth Predictions

S. Pommier

S. Pommier
LMT(ENS Cachan, CNRS, UPSaclay)

E-mail: Sylvie.pommier@universite-paris-saclay.fr

DOI : 10.12762/2015.AL09-11

Development of an Incremental Model for Fatigue Crack Growth Predictions

This paper presents an incremental approach for modeling fatigue crack growth with history effects. This approach is being developed at LMT since 2003, in collaboration with several industrial partners, mainly with Snecma, the SAFRAN Group, EDF and AREVA, and the SNCF. The first part of this paper presents the context, objectives and key assumptions on which the model is based. The second part presents some examples of applications of the model, fatigue crack growth under Mode I conditions, with variable amplitude loading; non-isothermal situations; crack growth under coupled environmental and fatigue loading conditions; extension of the model to non-proportional mixed mode loading conditions and to short cracks. The last part presents the ongoing work, the possible developments and the scientific challenges that remain to be overcome.

Introduction

Industrial sectors of public transportation (air, ground or naval) and of energy production (especially nuclear energy) implement an approach, called damage tolerance, to ensure that any damage located in a critical component will have limited consequences and will cause neither catastrophic failure in operating conditions nor fatalities. To do so, assumptions must first be made about the location, the geometry and the size of possible flaws in critical components. These assumptions depend on the resolution of non-destructive inspection techniques used before putting the system in operation or during preventive maintenance operations. If no damage has been detected, then the component is assumed to contain a non-detectable flaw. The design of the system and its preventive maintenance plan must ensure that this flaw will be harmless under operating conditions during the lifetime of the system. In order to do so, the most detrimental configuration is also assumed, i.e., the flaw is assumed to be a crack, located in the most critical zone of the component, with the worst possible orientation and with a size just below the detection threshold of the non-destructive inspection techniques used. At this point, models are needed to predict the growth of this potential crack, so as to predict the safe life of the component under operating conditions, to plan preventive maintenance operations, or the replacement of critical components or of the entire system. For a fail-safe approach, models are also needed to determine the crack path and the size of the fragments in the event of a sudden break, to predict the damage that they can cause and the consequences of the failure of a component on the behavior of the entire system.

However, accurate prediction of fatigue crack propagation and of the service life of critical components under operating conditions remains difficult for the following reasons:

- **2D / 3D**: Critical areas, where cracks are initiated, are usually stress concentration areas (notches, holes, contact areas, interfaces, thermal gradients, etc.), where the stress field usually exhibits a spatial gradient and may be multiaxial. This gives a three-dimensional character to the fatigue crack growth problem (short cracks, curved crack front, non-planar crack, or mixed mode loadings) [35,26]. However, the crack propagation models used to predict the growth of these 3D cracks usually use 2D experiments (Mode I, long and planar cracks).

- **Non-linear material behavior**: The materials used for critical components are, as far as possible, ductile materials and display a non-linear behavior. The non-linear nature of the behavior of the materials is at the origin of history or memory effects in fatigue crack growth. The importance of these history effects on fatigue crack growth has been demonstrated and explained [2, 16, 17, 18, 19, 20, 23, 28, 36, 40, 41, 47, 52, 53, 55, 56, 60, 61, 67, 68]. Various crack propagation models (NASGRO, PREFFAS, Strip Yield, etc.) have been developed to account for these history effects. If the material is non-linear, the loading path (not only the peak loads) is to be considered to predict the fatigue crack growth rate. However, since most models predict a fatigue crack growth rate per cycle, they require the use of a cycle counting method (e.g., rainflow) to be applied to load sequences under operating conditions that might be quite far from being cyclic. When the load sequence stemming from the cycle reconstruction differs significantly from the original one, the life prediction may be questionable. The incremental approach, which we have developed at LMT, avoids the use of a cycle reconstruction method by predicting a crack growth rate per second.

• **Other non-linear effects**: If any non-linear mechanism is involved, questions arise about cycle counting, damage accumulation, load path effects, etc. Aside from the non-linear material behavior, the primary source of nonlinearity is the interference between the crack faces, the plasticity or roughness induced crack closure problem in Mode I and the friction between the crack faces in Mode II and Mode III [4, 7, 8, 6, 12, 13, 14, 15, 21, 22, 24, 30, 39, 43, 51, 57]. Time dependent damage mechanisms may also contribute to crack growth (creep, corrosion, oxidation, etc.) and be coupled with pure fatigue crack growth. An incremental approach makes it possible to consider and to model independently the effects of each mechanism in each time step [1, 3, 5, 25, 29, 31, 34, 42, 49, 59, 65, 69, 70].

• **Complex loading conditions**: Loading sequences under actual operating conditions can be rather complex. The mechanical loadings can be uniaxial or multiaxial, varying in space and time (variable amplitude loading in Mode I, in-phase or out-of-phase loadings under mixed mode conditions, etc.). Similarly, it may be non-isothermal in space and time (thermal fatigue, etc.).

Since 2003, an incremental approach has been developed at LMT, step by step [9, 10, 11, 13, 21, 22, 27, 28, 38, 52, 53, 54, 55, 56, 59, 62], to predict fatigue crack growth under complex loading conditions and in non-linear materials. The approach is based on the assumption that “pure” fatigue crack growth stems from crack tip plasticity [37, 44, 45, 48]. With such an assumption, an incremental model for “pure” fatigue crack growth could be derived from an incremental plasticity model for the crack tip region. The crack growth rate per second can be predicted from the crack tip plasticity measurement. Various authors have derived successful predictions of the fatigue crack growth rate under complex loading conditions, from the analysis of the plastic strain field around the crack front obtained from non-linear finite element simulations. However, non-linear finite element simulations remain unusable in an industrial context, where cracks are usually 3D. A simplified model is required, but the finite element method can be used to develop a simplified model and to verify its capabilities.

The simplified model that has been developed at LMT is aimed at condensing all of the non-linear behavior effects of the material in the crack tip region into a set of constitutive equations based on the minimum number of variables necessary to reasonably represent the crack tip plasticity problem. Moreover, the simplifying assumptions in the model are chosen to be suitable with a use in mixed mode conditions.

Hypotheses

The model is based on some considerations that are briefly recalled below.

• Infinitesimal strain conditions are considered.

• The local solution is assumed to be dominated by the local geometry of the crack. The remote boundary conditions and their history are hence expected to control the intensity of the crack tip fields but not their spatial distribution, which is assumed to be given once for all, and to be associated with the local crack geometry.

• A curvilinear coordinate system R_T, defined with respect to a suitable characteristic scale, can be attached to the local crack front and the local crack plane. In this coordinate system R_T, the crack is assumed to be locally planar and under generalized plane strain conditions along the local straight crack front. This assumption allows the crack tip fields to be partitioned into Mode I (symmetric), Mode II (anti-symmetric) and Mode III (anti-planar) local components.

$$\underline{v}(P,t)_{R_0} = \underbrace{\underline{v}(T,t)_{R_0} + \omega(R_T / R_0) \wedge \underline{TP}}_{growth} + \underbrace{\underline{v}(P,t)_{R_T}}_{behaviour} \quad (1)$$

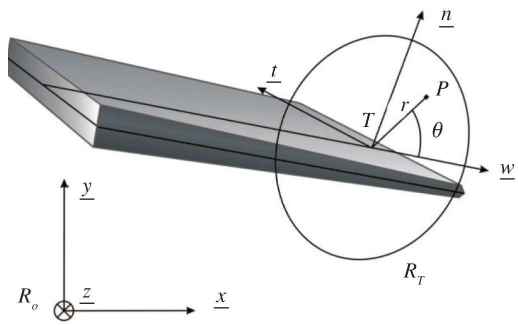

Figure 1 - Local coordinate system attached to the crack front (T) and plane

• With respect to the local coordinate system attached to the local crack plane and crack front, the geometry of the crack is locally scale invariant. This implies that, in each time step, the solution of the problem can be expressed (at least locally, in the vicinity of the crack front) as the product of an intensity factor and of a spatial distribution, which is scale invariant. It implies, in addition, that this spatial distribution can be expressed as the product of a function $f(r)$ of the scale (the distance to the crack tip r) and of a function $\underline{g}(\theta)$ of the angular position with respect to the crack plane. With this approach, the spatial distribution $f(r)\underline{g}(\theta)$ is given once for all and the intensity factor $I(t)$ can be considered as a degree of freedom.

$$\underline{v}(P,t)_{R_T} = \underline{v}(\underline{x},t) = I(t) f(r) \underline{g}(\theta) \text{ , where } f(\alpha r) = \beta f(r) \quad (2)$$

• Since it is always possible, at least transiently during a time step, to obtain a linear elastic behavior by reversing the loading direction (and assuming infinitesimal strain conditions), the elastic behavior of the crack tip region requires, for each mode, an independent degree of freedom even if elastic-plastic conditions are considered. In such a case, the hypotheses listed above apply independently to elastic and inelastic behaviors. If crack tip plasticity is well confined, the elastic bulk constrains the development of the crack tip plastic zone and this also drastically limits the number of useful degrees of freedom required to represent reasonably well the plastic flow obtained in the crack tip region.

This last property is illustrated in figure 2, for example. The accumulated plastic strain field obtained by elastic-plastic FE simulation under out-of-phase I+II mixed mode conditions was plotted in a logarithmic scale, for different points of a circular loading path in a KI-KII plane. At each point A, B, C or D, the angular distribution of P_{cum} is obviously the same whatever the distance r to the crack tip, so that $P_{cum} \propto f(r) g(\theta)$. In addition, it can be seen in figure 2 that P_{ti} decays exponentially from the crack tip, with the same decay rate throughout the mixed mode loading cycle.

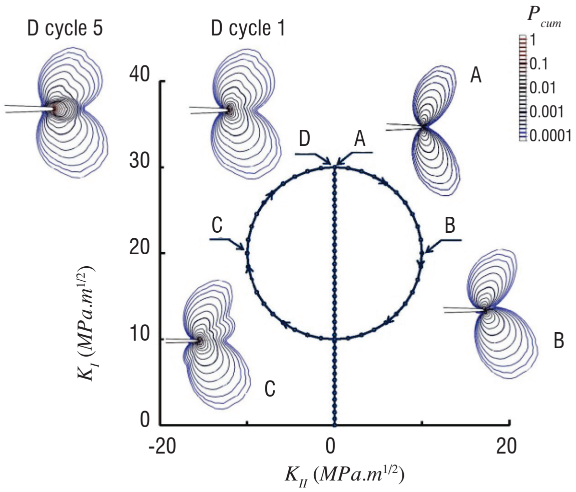

Figure 2 - Illustration : Five out-of-phase Mixed Mode I + II loading cycles (A-B-C-D) were simulated under non-linear conditions using the finite element method. The iso-values of the equivalent plastic strain P_{cum} are plotted in a logarithmic scale, during the first cycle in points A, B, C and D of the load path and at the end of the fifth cycle (D).

As a consequence, under elastic plastic conditions, the velocity field in a reference frame attached to the local crack tip and crack front can be approximated as the superposition of three modes, denoted by i. Each mode requires a degree of freedom $\dot{\tilde{K}}_i$ for the elastic response and another degree of freedom $\dot{\rho}_i$ for the inelastic one. Both the elastic and the inelastic part are expressed as the product of a spatial distribution and an intensity factor used as a degree of freedom and which can be calculated by post-processing elastic-plastic finite element results. The spatial distribution is constructed a priori and is the result of the various constraints (local crack geometry, symmetry, scale independence, etc.).

$$\underline{v}(P,t)_{R_T} = \sum_{i=1}^{3} \underbrace{\dot{\tilde{K}}_i(t).\underline{\varphi}_i^e(P)}_{\underline{v}_i^e(P,t)} + \underbrace{\dot{\rho}_i(t).\underline{\varphi}_i^c(P)}_{\underline{v}_i^c(P,t)} \tag{3}$$

$\underline{v}_i^c(P,t)$ represents the non-elastic part of the velocity field, while $\underline{v}_i^e(P,t)$ represents the elastic part.

If the material behavior is linear elastic, then the intensity factor $\dot{\tilde{K}}_i$ of the elastic part of the velocity field is equal to the nominal applied stress intensity factor $\dot{K}_i^\infty$. Otherwise, these two quantities are slightly different, because elastic strain may arise from applied stresses (and therefore from $\dot{K}_i^\infty$), but also from internal stresses arising from crack tip plasticity and from the confinement of the plastic zone. The difference ($\dot{\tilde{K}}_i - \dot{K}_i^\infty$) can be interpreted as the shielding effect of th plastic zone [58]. As expected, ($\dot{\tilde{K}}_i - \dot{K}_i^\infty$) was observed to be directly proportional to $\dot{\rho}_i$ by post-treatment of FE simulations.

The elastic reference fields $\underline{\varphi}_i^e(\underline{x})$ are obtained from a linear FE computation for each mode with $\dot{K}_i^\infty = 1MPa\sqrt{m}$ and fit the Westergaard solutions [66].

The non-elastic reference field $\underline{\varphi}_i^c(P)$ is obtained from elastic-plastic FE computations, using a model-reduction technique [32], as being the best possible field to approximate by Equation 3 the velocity field evolution calculated for each mode for a loading ramp from zero to 0.8 K_{Ic}. According to the model simplifying hypotheses, $\underline{\varphi}_i^c(P)$ can be locally represented by $f_i^c(r)\underline{g}_i^c(\theta)$ where $f_i^c(\alpha r)\beta f_i^c(r)$.

Assuming that the plastic zone is confined, this implies that $f_i^c(r) \underset{r\to\infty}{\to} 0$. And since $\underline{\varphi}_i^c(P)$ is the spatial distribution of the inelastic part of the velocity field at the crack tip, it should be discontinuous across the crack faces and maximum at the crack front, which implies that it should decay exponentially and which was observed in FE computations.

$$\begin{cases} f_i^c(\alpha r) = \beta f_i^c(r) \\ \quad f_i^c(r) \underset{r\to\infty}{\aleph} 0 \qquad f_i^c(r) \quad e^{-kr} \\ \quad f_i^c(r) \underset{r\to 0}{\to} 1 \end{cases} \tag{4}$$

$f_i^c(r)$ was rescaled to 1 when $r \to 0$, by convention. In addition, $\underline{g}_i^c(\theta)$ is discontinuous across the crack faces and was rescaled so that:

$$\left[\underline{g}_i^c(\theta)(\theta=\pi) - \underline{g}_i^c(\theta)(\theta=\pi)\right]_\theta = 1 \tag{5}$$

In practice, this post treatment is used to rescale each reference field $\underline{\varphi}_i^c(\underline{x})$ by a constant scalar value, so that the limit when r tends to zero of its discontinuity across the crack plane is equal to 1:

$$\left[\underline{\varphi}_i^c(\theta=\pi, r\to 0) - \underline{\varphi}_i^c(\theta=-\pi, r\to 0)\right]_\theta = 1 \tag{6}$$

In other words, the intensity factor $\dot{\rho}_I$ of $\underline{\varphi}_I^c(\underline{x})$ can now also be viewed as the CTOD, the intensity factor $\dot{\rho}_{II}$ of $\underline{\varphi}_{II}^c(\underline{x})$ as the Mode II CTSD and $\dot{\rho}_{ii}$ as the Mode III CTSD.

Details about the reference fields $\underline{\varphi}_i^e(P)$ and $\underline{\varphi}_i^c(P)$ and their construction for each mode can be found in previous papers [21, 54, 11].

With these assumptions, the crack tip field under non-linear mixed mode conditions can be fully characterized by only six independent degrees of freedom $\dot{K}_I^\infty$, $\dot{K}_{II}^\infty$, $\dot{K}_{III}^\infty$, and $\dot{\rho}_I$, $\dot{\rho}_{II}$, $\dot{\rho}_{III}$ and $\dot{\underline{\rho}} = (\dot{\rho}_I, \dot{\rho}_{II}, \dot{\rho}_{III})$ represents the discontinuity vector of the plastic velocity field across the crack face.

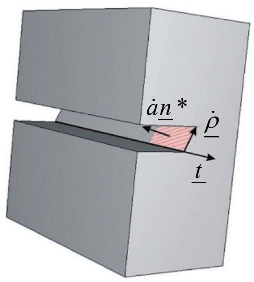

Figure 3 - Schematics of the process of creation of a new cracked area by crack tip plasticity (Neuman model [44, 45], Li model [37])

With such an approximation, following the approaches of Neuman [44, 45] and Li [37], the crack growth rate due to the geometric process of cracked area creation by plasticity can be estimated roughly as follows :

$$\dot{a}\underline{n}^* \propto \left(\underline{t} \wedge \dot{\underline{\rho}}\right) \Rightarrow \dot{a} \propto \sqrt{\dot{\rho}_I^2 + \dot{\rho}_{II}^2} \tag{7}$$

Where $\underline{t}$ is the unit orientation vector of the crack front, $\underline{n}^*$ is the unit vector normal to the cracked face oriented outward and $\dot{a}$ is the rate of cracked area creation per unit length of the crack front. It is worth emphasizing that, with such an assumption, Mode III plastic flow in the crack tip region has no effect on the crack growth rate. This point is discussed in § "Mixed mode loading conditions", since Mode III is known to contribute to fatigue crack growth [50, 63].

Once the basis of the reference field has been determined, it can be used to post-process velocity fields obtained from finite element simulations or from experimental field measurements from digital image correlation [11].

The velocity field $\underline{\ddot{u}}^{\ddot{u}}$ (,) recorded at each time step is projected onto the six reference fields, in order to retrieve the intensity factors related to the elastic and the inelastic parts for each mode:

$$\dot{\tilde{K}}_i(t) = \frac{\int \underline{v}^{rec}(P,t).\underline{\varphi}_i^e(P)\mathrm{dP}}{\int \underline{\varphi}_i^e(P).\underline{\varphi}_i^e(P)\mathrm{dP}} \quad , \quad \dot{\rho}_i(t) = \frac{\int \underline{v}^{rec}(P,t).\underline{\varphi}_i^c(P)\mathrm{dP}}{\int \underline{\varphi}_i^c(P).\underline{\varphi}_i^c(P)\mathrm{dP}} \tag{8}$$

In order to quantify the quality of the approximation in equation 3, the error $C_{2R}(t)$ is also determined in each time step:

$$C_{2\mathrm{R}}(t) = \sqrt{\frac{\int \left(\underline{v}^{rec}(P,t) - \dot{\tilde{K}}_i(t)\underline{\varphi}_i^e(P) - \dot{\rho}_i(t)\underline{\varphi}_i^c(P) \right)^2 \mathrm{dP}}{\int \left(\underline{v}^{rec}(P,t) \right)^2 \mathrm{dP}}} \tag{9}$$

This error is usually below 10% but increases drastically when the crack is no longer under small scale yielding conditions or when contact occurs between the crack faces. In order to quantify the importance of the plastic part of the approximated velocity field, the error $C_{1R}(t)$ is also determined in each time step:

$$C_{1\mathrm{R}}(t) = \sqrt{\frac{\int \left(\underline{v}^{rec}(P,t) - \dot{\tilde{K}}_i(t)\underline{\varphi}_i^e(P) \right)^2 \mathrm{dP}}{\int \left(\underline{v}^{rec}(P,t) \right)^2 \mathrm{dP}}} \tag{10}$$

If $\left| C_{1R}(t) - C_{2R}(t) \right|$ is very small, it means that adding a plastic part to the approximation in Equation 3 does not improve it; the behavior of the crack tip region is thus essentially elastic during the time step. This criterion was used to define the frontier of the elastic domain under mixed mode conditions.

Applications and ongoing work

A very small number of degrees of freedom can hence be used to represent the kinematics of the crack tip region reasonably well. Numerical simulations (or experiments with full field measurement) can be used to determine the velocity field and to track the evolution of $\dot{\rho}_i$ for various loading conditions $\dot{K}_i^\infty$, so as to derive a constitutive model of the non-linear behavior of the crack tip region.

The approach used to develop the model is analogous to that used for many years by the Mechanics of Materials community to develop material laws with internal variables within a thermodynamic framework. However, it should be noted that:

- The constitutive law applies to a region and not to a material point. The approach is hence non-local and is tailored for the crack tip region through the use of the reference fields $\underline{\varphi}_i^e(P)$ and $\underline{\varphi}_i^c(P)$ that include a discontinuity across the crack faces.

- Internal variables are introduced to account for the existence of internal stresses, of material hardening and more generally of any other effect related to the non-linear behavior of the material that could be at the origin of significant memory effects in fatigue crack growth. However, the constitutive law for the crack tip region, and hence the internal variables of this constitutive law, are inherent to the crack front, not to the material. Consequently, the internal variables of the constitutive model of the crack tip region will not only have to evolve with plastic flow within the crack tip region, but also as a result of the crack front displacement.

- Due to the presence of the crack in the crack tip region, plastic flow is localized from the beginning and must remain localized in the same manner, as long as the plastic zone is confined by the elastic bulk. Thus, we are spared many difficulties related to the issue of accounting for the localization process or the post-peak transition in the constitutive model.

- From a thermodynamic point of view, the driving force associated with $\dot{\rho}_i$ is not the nominal applied stress intensity factors, but rather $\varphi_{\ddot{u}} = \frac{1-v^2}{E} sign\left(K^\infty\right) K^{2\infty}$. Nevertheless, for ease of reading, the model equations are written in terms of K_i^∞.

The constitutive model for the plasticity of the crack tip region is then associated with a crack propagation model to obtain the incremental model. In "pure" fatigue, the rate $\dot{a}$ of production of cracked areas per unit length of crack front is given by the plastic flow rate $\dot{\rho}_i$: $\dot{a} = \alpha \sqrt{\dot{\rho}_I^2 + \dot{\rho}_{II}^2}$.

Mode I fatigue crack growth

Early work was carried out on modeling fatigue crack growth in Mode I at room temperature under variable amplitude loading [55, 56] for aircraft engine applications and then for railway applications [27, 28, 53]. Then, the model was extended to modeling fatigue crack growth under non-isothermal conditions and in the presence of an active environment [59].

Attempts have also been made to extend the model to elastic-viscoplastic materials, with promising results. Studies in this direction have been conducted as part of a collaboration with the University of Sao Paulo, Brazil (PhD thesis of M. Angeloni) and during the Masters internship of P. Nam Wong (Snecma).

A set of constitutive equations was defined that allows $d\rho_I$, the plastic flow in Mode I in the crack tip region, to be determined as a function of the Mode I nominal applied stress intensity factor dK_I^∞.

The model is based on two elastic domains, one for the cyclic plastic zone and the other for the monotonic plastic zone. Each of them is characterized by two internal variables that represent, respectively, the center $\left(K_x^{cpz} \text{ and } K_x^{mpz}\right)$ and the size $\left(K_x^{cpz} \text{ and } K_x^{mpz}\right)$ of each elastic domain.

Results such as that plotted in figure 4 can be obtained using the finite element method, either for a fixed position of the crack front to obtain $\frac{\partial V_{\text{int}}}{\partial \rho_I}$, or after numerically "growing" the crack without allowing plastic strain, so as to obtain $\frac{\partial V_{\text{int}}}{\partial \rho_a}$. This allows an evolution equation to be determined independently for each internal variable, due to plasticity $\frac{\partial V_{\text{int}}}{\partial \rho_I}$ or due to crack propagation $\frac{\partial V_{\text{int}}}{\partial \rho_a}$. The evolution equations introduced for each internal variable are empirical.

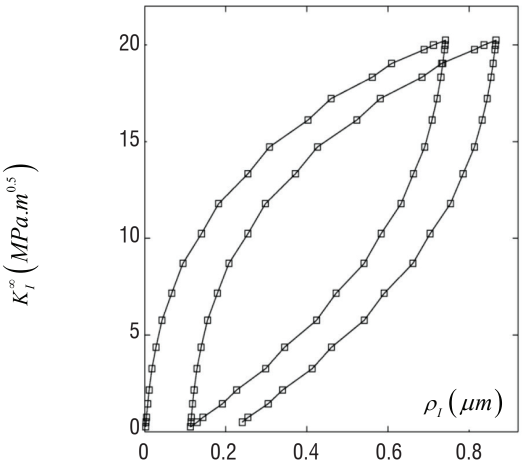

Figure 4 - Illustration of the evolution of the Mode I plastic intensity factor as a function of the Mode I nominal applied stress intensity factor K_I^∞ [10]

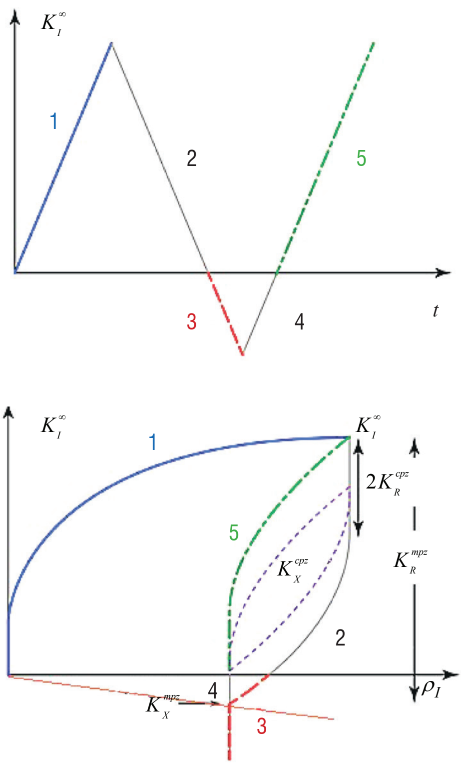

Figure 5 - Illustration of the evolution of the role of each internal variable used in the model

Cyclic plastic zone - K_R^{cpz}

For the cyclic plastic zone, the size of the elastic domain K_R^{cpz} was assumed to be constant. The material constitutive laws that were used for most simulations (Figure 4) included both non-linear kinematic and isotropic hardening [36]. However, the effect of isotropic hardening that is expected to be produced and the evolution of K_R^{cpz} were usually observed to be small and neglected up to now.

Fatigue crack growth is assumed to be the result of crack tip plasticity, through the crack growth model $\dot{a} = \alpha\sqrt{\dot{\rho}_I^2}$, therefore the fatigue threshold ΔK_{th} predicted by the model is equal to $2K_R^{cpz}$.

Cyclic plastic zone - K_x^{cpz}

The evolution law of the center of the elastic domain K_x^{cpz} due to plasticity $\frac{\partial K_x^{ü}}{\partial \rho_I}$ is determined from numerical results, such as those depicted in figure 4, for example.

We first proposed an equation that fits the numerical results as well as the numerical results (a power low function with a threshold), but then we preferred to make sure that a unique set of material parameters could be identified, so that we could be able to interpolate the parameters identified for different temperatures, for example. Finally, we also added the constraint that the evolution equations of each internal variable, with respect to plastic flow $\left(\partial\rho_I\right)$ or with respect to the displacement of the crack front $\left(\partial a\right)$, would be consistent, so that:

$$\frac{\partial}{\partial a}\left(\frac{\partial K_x^{cpz}}{\partial \rho_I}\right) = \frac{\partial}{\partial \rho_I}\left(\frac{\partial K_x^{cpz}}{\partial a}\right)$$

Once $\frac{\partial K_x^{cpz}}{\partial \rho_I}$ and K_x^{cpz} are identified from finite element computations (including the constitutive law of the material), the amplitude $\Delta\rho_I$ per fatigue cycle can be predicted as a function of ΔK_I^∞ for a given material. Since we also assume that $\dot{a} = \alpha\sqrt{\dot{\rho}_I^2}$, the fatigue crack growth rate can hence be determined $\frac{da}{dN} = 2\alpha\Delta\rho_I$. It is worth noting that a fatigue crack growth experiment is necessary to adjust the coefficient. In a Paris diagram, this coefficient α allows the position of the Paris law to be adjusted, but not its slope. The slope of the Paris law and the predicted fatigue threshold ΔK_{th}, stem from the relation between ΔK_I^∞ and $\Delta\rho_I$, which are identified, using the finite element method on the basis of the elastic-plastic constitutive behavior of the material.

Monotonic plastic zone - K_R^{mpz}

The size ^{mpz} of the elastic domain in Mode I is directly related to the size of the plastic zone. As a matter of fact, the intensity factor of the plastic part of the velocity field is $\dot{\rho}_I$. It decays exponentially with the distance from the crack tip. Therefore, for a monotonic loading ramp the evolution of ρ_I as a function of K_I^∞ is directly related to the growth of the plastic zone size with K_I^{∞}. In addition, an exponential decay is chosen for $\frac{\partial K_R^{mpz}}{\partial a}$.

Monotonic plastic zone - K_x^{mpz}

The center K_x^{mpz} of the elastic domain in Mode I is also defined as the contact point between the crack faces, whose evolution with crack tip plasticity $\frac{\partial K_x^{mpz}}{\partial \rho_I}$ can be determined using the finite element method. When crack tip blunting occurs $(d\rho_I>0)$, the crack opening level decreases.

The evolution of K_x^{mpz} with the crack length allows the crack closure effect to be accounted for. As the crack propagates through the plastic zone, the internal stresses stored in the plastic zone are transferred from the ligament to the crack faces, resulting in an increase of K_x^{mpz} that is modeled as being proportional to the internal stresses stored in the crack tip region and hence to the plastic zone size. Then, once internal stresses have entirely been transferred to the crack wake, their distance to the crack tip increases with the extent of the crack, producing a decrease in the crack opening level. This yields the empirical equation 11:

$$\frac{\partial K_X^{mpz}}{\partial a} = k_b K_R^{mpz} - k_a K_X^{mpz} \tag{11}$$

Applications – variable amplitude fatigue

The equations were implemented and their coefficients identified using the finite element method for a low carbon steel, by Rami Hamam [27, 28, 53]. The coefficient α of the crack propagation law $\dot{a} = \alpha\sqrt{\dot{\rho}_I^2}$ was adjusted using a Mode I fatigue crack growth experiment in constant amplitude fatigue at $R=0$.

Then, the model was used to simulate the stress ratio effect, the overload effect and the effects of various block loadings on fatigue crack growth [27, 28, 53]. The simulations were compared to experimental results giving satisfactory results. It was shown that the model is capable of representing the stress ratio effect, the overload effect, the overload retardation effect, the higher retardation effect after 10 overloads than after one single overload, etc.

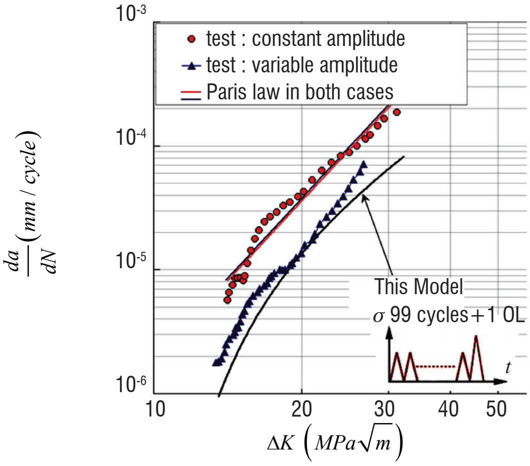

Figure 6 - Illustration of the capability of the model to predict the retardation effect of one overload, with an overload factor of 1.3, in a block of 100 cycles

Applications – non-isothermal conditions and environmental effect

In order to extend the model to non-isothermal conditions, Juan Antonio Ruiz Sabariego [59] identified the parameters of the constitutive model for the N18 nickel base superalloy at various temperatures between 450°C and 650°C. Finite element computations were then performed, in order to identify the parameters of the constitutive law of the crack tip region as a function of the temperature. The parameters obtained for each temperature were interpolated so as to obtain a plasticity model for the crack tip region under non-isothermal conditions [59].

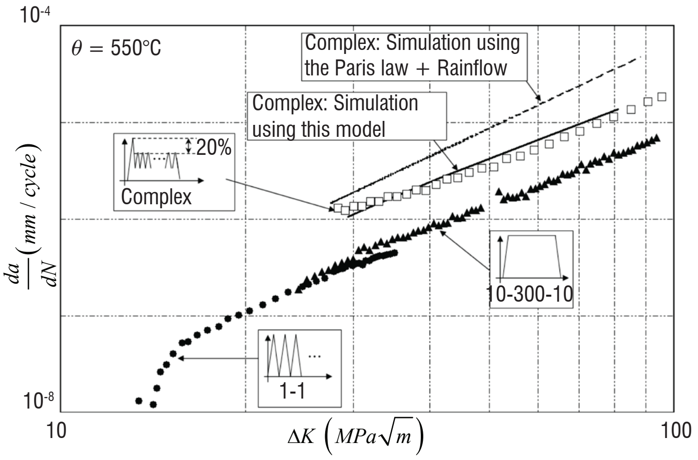

Figure 7 - Fatigue crack growth rate in CT specimens at 550°C in the N18 nickel base superalloy. Symbols correspond to experiments and lines to predictions [59]

In addition, the phenomenon of oxidation that assists fatigue crack growth at high temperatures [49, 3, 33, 31, 70, 64, 29] must also be considered. This mechanism is responsible, for instance, for the detrimental effect of dwell times at temperatures above 550°C [29, 5, 69, 34] in the N18 nickel base superalloy. The grain boundaries are embrittled by oxidation ahead of the crack tip. This mechanism is thermally activated. In addition, the material is designed to develop a passivation layer of oxides, which protects the material against grain boundary oxidation. However, if the crack tip is stretched, the passivation layer breaks and a competition between grain boundary embrittlement and the growth of a passivation layer takes place. Therefore a coupling effect between fatigue and oxidation is observed. This explains, in particular, why the crack growth rate is not only sensitive to the duration of the fatigue cycle, but also to its shape.

These phenomena are modeled as follows. The crack growth rate is now the sum of two terms, the first term is due to crack tip plasticity (Eq. 3), while the second term accounts for the contribution of the time during which grain boundary oxidation takes place:

$$\frac{\mathrm{da}}{dt} = \frac{\partial \mathrm{a}}{\partial \rho_I}\frac{d\rho_I}{dt} + \frac{\partial \mathrm{a}}{\partial t} = \underbrace{\alpha\left|\frac{d\rho_I}{dt}\right|}_{pure\ fatigue} + \underbrace{\frac{\partial \mathrm{a}}{\partial t}}_{oxydation} \tag{12}$$

The cyclic elastic-plastic constitutive model for the crack tip region, which provides $\frac{d\rho_I}{dt}$, is a function of the temperature through the dependency of the material cyclic elastic-plastic behavior on the temperature. In addition, the adjustable parameter α was determined using fatigue crack growth experiments at rather high frequency, for which the contribution of the environment is assumed to be negligible (1-1 cycles).

The second term of this equation (Eq. 12) corresponds to the contribution of grain boundary embrittlement by the chemical environment to the fatigue crack growth. Simple partial derivative equations were used to represent the mechanisms of embrittlement identified by other authors [29, 5, 69, 34]. Since grain boundary embrittlement stems from a diffusion process, it was assumed to be thermally activated (Eq. 13).

$$\frac{\partial a}{\partial t} = m\beta_o exp\left(-\frac{Q}{kT}\right) \tag{13}$$

The crack growth rate $\beta_0 exp\left(-\frac{Q}{KT}\right)$ by grain boundary embrittlement, in the absence of any passivation layer, is modulated by the variable m, which represents the state of that passivation layer. When $m=1$, the passivation layer is broken and the crack growth rate by grain boundary embrittlement is maximum. When $m=2$, the passivation layer is thick enough to fully protect grain boundaries against oxidation. Two adjustable parameters are introduced, in order to control the variations of m. The parameter R_G is introduced, to represent the growth rate of that passivation layer versus time; the parameter R_F is introduced so as to model how the rupture of the oxide layer increases the crack growth rate by grain boundary embrittlement. It is assumed that the oxide layer breaks when the crack tip is stretched, because of crack tip plasticity. This happens only at the opening, when $d\rho_I$ is positive.

$$\begin{cases} \dfrac{\partial m}{\partial t} = -R_G m \\ \dfrac{\partial m}{\partial \rho_I} = -R_F\left(1-m\right), \quad with\ d\rho_I > 0 \end{cases} \tag{14}$$

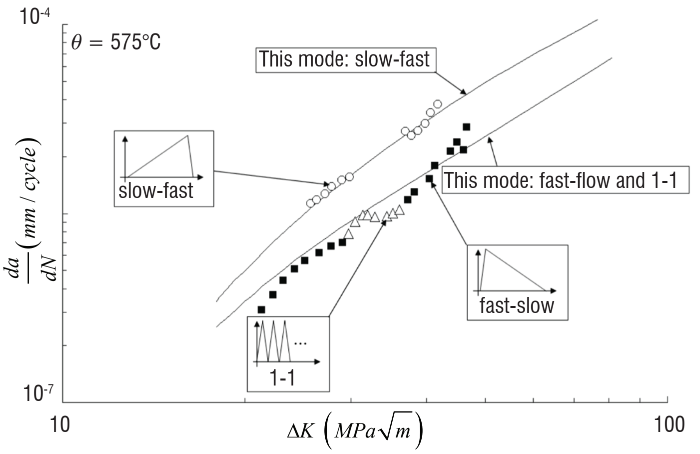

Figure 8 - Fatigue crack growth rate in CT specimens at 575°C in the N18 nickel base superalloy. Symbols correspond to experiments conducted by Hochstetter et al [29] and lines correspond to predictions by the incremental model [59].

This model was validated using complex isothermal fatigue crack growth experiments. For instance, it was possible to reproduce the difference between fast-slow and slow-fast fatigue crack growth experiments (figure 7) [29, 59]. This result was also satisfactory because the parameters were identified at 450°C, 550°C, 600°C and 650°C. 575°C is an intermediate temperature that was not used for the identification. It also successfully reproduces the effect of the shape of the fatigue cycle that was observed in the experiments, though this type of cycle was never used during the identification phase.

Mixed mode loading conditions

The model was then extended to the case of fatigue crack growth under Mixed Mode I + II, loading conditions [10, 11, 54] and for the general case of mixed-mode (I + II + III) loading conditions [21, 22]. P.Y Decreuse [10, 11, 54] and Flavien Fremy [21, 22] have clearly demonstrated, through fatigue crack growth experiments for Mixed Mode I + II and I + II + III on the Astree platform of the LMT, the importance of the load path effect in steel alloys to predict both the crack growth rate and the crack path.

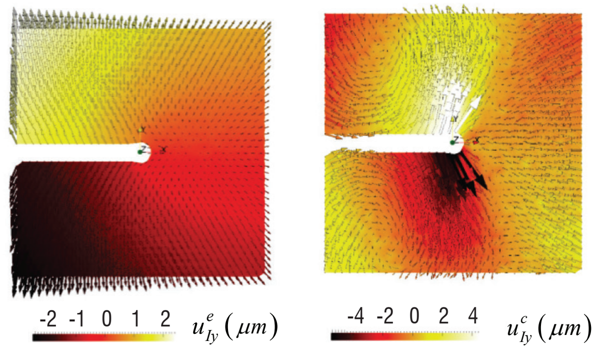

(a) (b)

Figure 9 - Mode I reference fields constructed using DIC. Intensity of the component normal to the crack plane. (a) Elastic reference field, (b) Non-elastic reference field.[10]

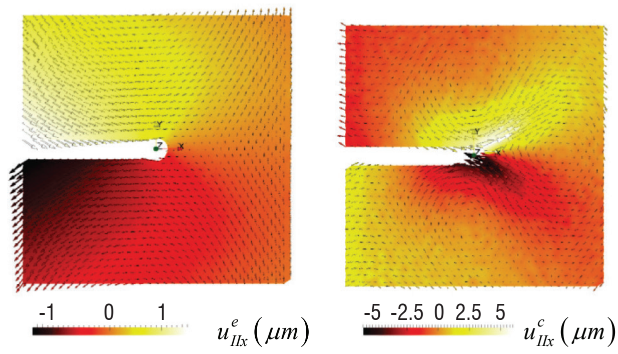

(a) (b)

Figure 10 - Mode II reference fields constructed using DIC. Intensity of the component parallel to the crack plane. (a) Elastic reference field, (b) Non-elastic reference field.[10]

Experimental velocity fields recorded using digital image correlation were post-treated, as explained in Section 2. The experimental reference fields are consistent with those obtained by FE simulations under mixed mode conditions.

It was also possible to determine the evolution $\dot{\rho}_I$ and $\dot{\rho}_{II}$ of the plastic intensity factors as a function of the nominal applied stress intensity factor rates $\dot{K}_I^\infty$ and $\dot{K}_{II}^\infty$. The experimental results confirmed the hypotheses of the model.

Experiments were conducted under Mode I+II and Mode I+II+III non-proportional loading conditions, in order to characterize the load path effect in fatigue crack propagation in 316L stainless steel and the contribution to fatigue crack growth of Mode III loadings [21, 22]. The same maximum, minimum and mean values of the stress intensity factors were used for each loading path in the experiments. Since the same maximum, minimum and mean values of the stress intensity factors were applied in each experiment, the load paths are all considered to be "equivalent" with respect to most of the fatigue crack growth criteria, in particular with respect to those based on $\Delta K_{eq} = \left(\Delta K_I^n + \beta \Delta K_{II}^n + \gamma \Delta K_{III}^n \right)^{1/n}$.

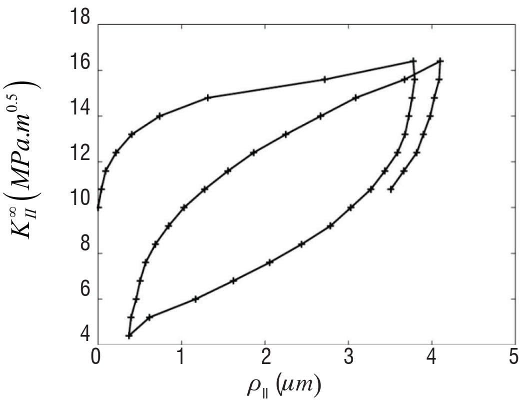

Figure 11 - Evolution of the CTSD as a function of the Mode II nominal applied stress intensity factor. Measurement performed using digital image correlation (DIC), during a Mode II loading phase $\Delta K_{II}^{\infty} = 12 MPa\sqrt{m}$ around a mean value $\left(K_{II}^{\infty} = 30 MPa\sqrt{m}, K_{II}^{\infty} = 0 \right)$.[10]

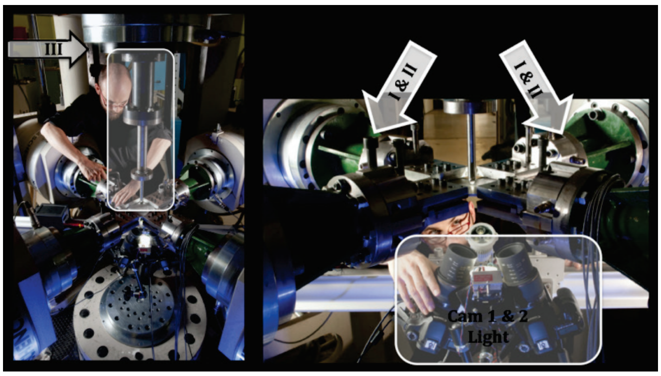

(a)

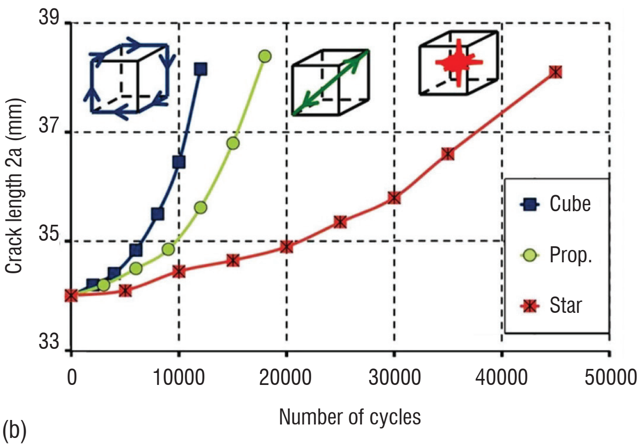

(b)

Figure 12 - (a) Experimental set-up -Six actuator servo-hydraulic testing machine ASTREE, (b) crack length evolution for three Mixed Mode I+II+III cases for which $\Delta K_I = \Delta K_{II} = \Delta K_{III}$. The three modes were either applied simultaneously (circles), or sequentially (cube), or one after the other (star). [21, 22]

The experiments were conducted on the multiaxial servo-hydraulic testing machine ASTREE, available at LMT. Six actuators were used simultaneously to perform the tests (figure 12). Three pairs of actuators were used to load the specimen along three orthogonal axes and to keep the intersection of the three loading axes fixed. Each horizontal loading axis was load controlled.

The main result of this set of experiments is that very different crack growth rates are observed even though the extreme values and the mean values of the stress intensity factors are the same in each test. A variation by up to a factor of three for the crack growth rate according to the loading path was observed in these experiments, even when the crack path remained macroscopically coplanar. In addition, it was shown that the crack path is also significantly dependent of the load path. For instance, the crack path remains coplanar for the "square" load path, while a tilt is observed for the "proportional" load path in Mixed Mode I+II. In these two cases, the extreme values of the Mode I and Mode II stress intensity factors are attained simultaneously.

Elastic plastic finite element analyses were conducted, in order to analyze, at the scale of the crack tip region, the load path effect on plastic flow under Mixed Mode I+II+III conditions (i.e. $\dot{\underline{\rho}} = (\dot{\rho}_I, \dot{\rho}_{II}, \dot{\rho}_{III})$). The load paths tested in these simulations were identical to those used in experiments. By considering that the crack growth rate could be roughly estimated from the Mode I+II parts of the plastic flow rate within the crack tip region, it was possible to show that different load paths displaying the same stress intensity factors for each mode would nevertheless produce different plastic flow amplitudes and hence different crack growth rates.

The finite element simulations were consistent with the experiments, since it was possible to discriminate between the most and the least detrimental load paths and to predict the order of magnitude of the load path effect.

Finally, it was also shown that the mode mixity of the plastic flow rate within the crack tip region does not coincide with the mode mixity of the nominal applied stress intensity factor rate (figure 13). In particular, the addition of a Mode III stress intensity factor amplitude to a Mode I+II cycle increases the Mode I+II plastic flow amplitude in the cycle.

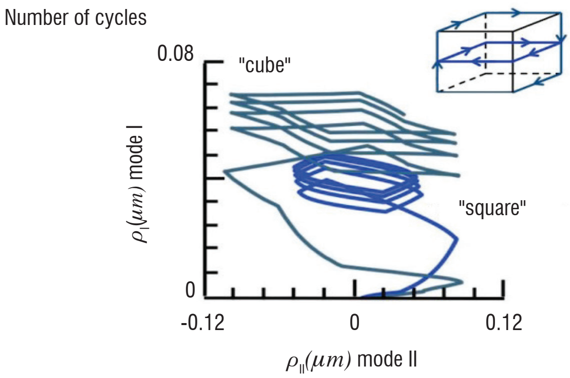

Figure 13 - Mode I+II plastic flow, as calculated from FE analyses, for the "square" and "cube" load paths. The plastic flow amplitude in Mixed Mode I+II is increased when a Mode III stress intensity factor amplitude is added to a Mode I+II load cycle. [22]

A model for mixed mode plasticity was introduced and was the subject of the PhD thesis of F. Fremy in Mode I+II+III [21, 22] and of P. Y. Decreuse in Mode I+II [10, 11, 54]. The model predicts the evolutions of the plastic intensity factor under variable amplitude and non-proportional mixed mode conditions, and the plasticity rates predicted by the model under complex conditions are consistent with crack growth rates obtained in the experiments.

At the moment, the model under Mixed Mode I+II+III conditions contains only one elastic domain for the cyclic plastic zone. It was able to successfully predict the load path effect in constant amplitude fatigue (in phase / out of phase, proportional versus square versus star cycles). However, in order to predict the overload effect, for example, a second elastic domain for the monotonic plastic zone would be useful.

The plasticity model for the crack tip region under Mixed Mode I+II+III conditions contains three components:

- A yield function
- A normality flow rule
- A kinematic hardening rule

The yield criterion was obtained by considering that the yield condition is reached under mixed-mode conditions for the same critical distortional elastic energy as in Mode I. It is then analogous to the Von Mises criterion, except that instead of being applied to a material point, it is applied to the entire crack tip region. To some extent, it is a non-local Von Mises criterion tailored to cracks. To do so, the distortional elastic energy density was calculated under mixed mode conditions using the Westergaard stress functions [66] and then integrated over a domain with a radius D around the crack tip. Given that the Westergaard stress functions [66] of each mode depend on the distance to the crack tip in the same way, the critical distortional elastic energy criterion is not dependent on D and can be reduced to:

$$f = \frac{\left(K_I^\infty - K_I^X\right)^2}{\left(K_I^Y\right)^2} + \frac{\left(K_{II}^\infty - K_{II}^X\right)^2}{\left(K_{II}^Y\right)^2} + \frac{\left(K_{III}^\infty - K_{III}^X\right)^2}{\left(K_{III}^Y\right)^2} - 1$$

where $K_{II}^Y = K_I^Y \sqrt{\frac{7-16\nu(1-\nu)}{19-16\nu(1-\nu)}} \approx 0.48\, K_I^Y$

and $K_{III}^Y = K_I^Y \sqrt{\frac{7-16\nu(1-\nu)}{24}} \approx 0.39\, K_I^Y$

or

$$f\left(G_I, G_{II}, G_{III}\right) = \frac{|G_I|}{G_I^Y} + \frac{|G_{II}|}{G_{II}^Y} + \frac{|G_{III}|}{G_{III}^Y} - 1$$

where $G_i^Y = \frac{1-\nu^2}{E}\left(K_i^Y\right)^2$

and $G_i = signe\left(K_i^\infty - K_i^X\right)\frac{1-\nu^2}{E}\left(K_i^\infty - K_i^X\right)^2$

This criterion was shown to be consistent with finite element computations and also, in Mixed Mode I+II, with results obtained using digital image correlation.

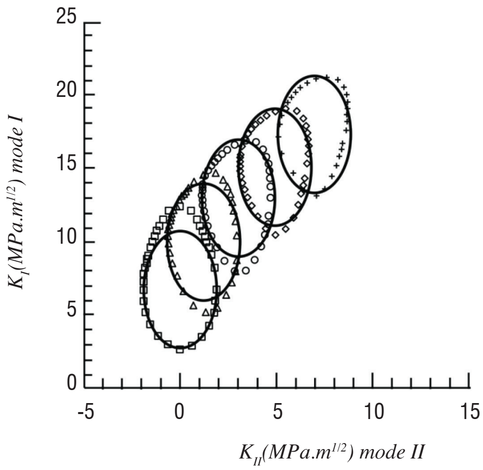

Figure 14 - Evolution of the yield surface during a Mixed Mode I+II loading ramp. The symbols corresponds to the yield points determined from FE computations using the C_{1R}-C_{2R} numerical criterion (Eqs. 9 & 10), the solid lines correspond to the yield function based on a critical distortional energy [54].

The size of the elastic domain is still assumed to be a constant and the shape of the elastic in a K_I, K_{II}, K_{III} diagram is an ellipsoid, whose aspect ratios are a function of the Poisson ratio of the material.

The center of the elastic domain is allowed to be displaced along the plastic flow direction $\underline{\dot{\rho}} = \left(\dot{\rho}_I, \dot{\rho}_{II}, \dot{\rho}_{III}\right)$. In addition, the plastic flow direction is assumed to be normal to the yield function in terms of G_i.

The model was shown to be able to reproduce the evolution of the plastic flow intensity factors calculated using mixed mode elastic plastic FE computations, when complex loading conditions where applied.

Conclusions and future work

An approach was proposed to model the non-local elastic-plastic behavior of the crack tip region. This approach is based on an approximation of the kinematics of the crack tip region. To some extent, it is a non-local elastic plastic constitutive model, tailored to a crack tip region.

The use of this model makes it possible to enrich the usual linear elastic fracture mechanics functions by additional terms that are capable of accounting for the cyclic elastic-plastic behavior of the material, including history effects. The model is valid only under small scale yielding conditions and is dedicated to predicting fatigue crack growth under complex loading conditions (variable amplitude loading, non-isothermal conditions, etc.).

The model provides a scalar measurement of the amount of plastic flow for each mode during a time step, as a function of the loading step (given in terms of the stress intensity factors for each mode). The parameters of the model can be identified using the constitutive law of the material and finite element computations of the behavior of the crack tip region. This model is a non-linear constitutive law for the crack tip region, with internal variables to account for memory effects. A temperature dependency of its parameters can be defined, in order to use it under non-isothermal conditions.

Thus, the rate of production of cracked areas during a time step, due to pure fatigue, is assumed to be directly proportional to the amount of plastic flow predicted by the model. Other mechanisms (oxidation, corrosion) can be also considered and added to the crack propagation law if necessary.

The constitutive model for the crack tip region and the crack propagation law, together, are an incremental model for fatigue crack growth.

In Mode I, the model was completely identified for predicting fatigue crack growth under mixed mode conditions and validated using a large set of experiments. It was extended to non-isothermal conditions and the crack propagation law was completed to include a contribution of oxidation to crack growth. The model simulations were compared to experimental results giving satisfactory results.

Under mixed mode conditions, the model was partially developed and was shown to be able to predict the load path effect successfully under mixed mode conditions. It also provides a framework to analyze mixed mode fatigue tests, in particular the role of Mode III on fatigue crack growth.

The model requires additional development to be able to predict the overload effect under mixed mode conditions. This would not require extensive numerical or modeling work, but the validation by means of experiments would require significant effort. In addition, the prediction of the crack path under mixed mode conditions requires further work. Ongoing work is aimed at extending the validity domain of the model to short cracks by including the T-stresses and to large scale yielding conditions

Acknowledgements

I would like to warmly acknowledge the PhD students and Post Doctorates who contributed directly to the development of this model, or that are developing it, Marion Risbet, Rami Hamam, Juan Antonio Ruiz Sabariego, Pablo Lopez Crespo, Pierre-Yves Decreuse, Sophie Dartois, Flavien Fremy, François Brugier and Wen Zhang. Also, I would like to acknowledge our industrial partners for their constant support and interest, Snecma, EDF and AREVA, SNCF and the DGA. In addition, I would also like to acknowledge all of my colleagues for fruitful discussions, Veronique Doquet, François Hild, Ahmed Benallal, Rodrigue Desmorat, Antony Gravouil, Bertrand Burgardt, Didier Soria, Marie Christine Baietto and many others.

References

[1] M.R. HTER, G.J.DANEK, H.H. SMITH - *Effect on Fatigue of Gaseous Environments Under Varying Temperature and Pressure.* Trans. Metall. Soc. AIME, 227(December), 1296–1301, 1963

[2] D. ALIAGA - *Prevision de la fissuration en fatigue sous chargements d'amplitude variable*. Modele PREFFAS, Aerospatiale, Laboratoire Central Doc. PV. No. 47.904, (1985).

[3] J-L. BOUVARD - *Modélisation de la propagation de fissures dans les aubes de turbine monocristallines.* Thesis of ENSMP, Paris, 2006

[4] M.W.B. BROWN, S. L. WONG, et al. (2000) - *Fatigue Crack Growth Rates under Sequential Mixed-Mode I and II Loading Cycles.* Fatigue & Fracture of Engineering Materials & Structures 23(8): 667-674.

[5] J-C. CHASSAIGNE - *Fissuration à hautes temperatures du superalliage base nickel N18 élaboré par métallurgie des poudres, étude du couplage mécanique-environnement en pointe de fissure.* Thèse de l'Ecole Nationale Supérieure des Mines de Paris, 1997

[6] B. H. CHOI, J. M. LEE (2009) - *Experimental Observation and Modeling of the Retardation of Fatigue Crack Propagation under the Combination of Mixed-Mode Single Overload and Constant Amplitude Loads.* International Journal of Fatigue 31(11-12): 1848-1857.

[7] P. DAHLIN, M. OLSSON (2004) - *Reduction of Mode I Fatigue Crack Growth Rate Due to Occasional Mode II Loading.* International Journal of Fatigue 26(10): 1083-1093.

[8] P. DAHLIN, M. OLSSON (2006) - *Mode I Fatigue Crack Growth Reduction Mechanisms After a Single Mode II Load Cycle.* Engineering Fracture Mechanics 73(13): 1833-1848.

[9] P.Y. DECREUSE, S. POMMIER, M. PONCELET, B. RAKA(2011) - *A Novel Approach to Model Mixed Mode Plasticity at Crack Tip and Crack Growth. Experimental Validations Using Velocity Fields from Digital Image Correlation.* International Journal of Fatigue

[10] P.Y. DECREUSE, S. POMMIER, L. GENTOT, S. PATTOFATTO - *History Effect in Fatigue Crack Growth under Mixed Mode Loading Conditions.* Int. J. Fatigue, vol. 31, pp. 1733–1741, (2009)

[11] P.Y. DECREUSE, S. POMMIER, M. PONCELET, B. RAKA - *A Novel Approach to Model Mixed Mode Plasticity at Crack Tip and Crack Growth. Experimental Validations Using Velocity Fields from Digital Image Correlation.* Int Jal of Fatigue. 2011 http://dx.doi.org/10.1016/j.ijfatigue.2011.11.021.

[12] V. DOQUET, G. BERTOLINO (2008) - *Local Approach to Fatigue Cracks Bifurcation.* International Journal of Fatigue 30(5): 942-950.

[13] V. DOQUET, S. POMMIER (2004) - *Fatigue Crack Growth under Non-Proportional Mixed-Mode Loading in Ferritic-Pearlitic Steel.* Fatigue & Fracture of Engineering Materials & Structures 27(11): 1051-1060.

[14] V. DOQUET, Q.H. BUI, A. CONSTANTINESCU (2010) - *Plasticity and Asperity-Induced Fatigue Crack Closure under Mixed-Mode Loading.* International Journal of Fatigue, Vol. 32, pp. 1612-1619.

[15] V. DOQUET, M. ABBADI, et al. (2009) - *Influence of the Loading Path on Fatigue Crack Growth under Mixed-Mode Loading.* International Journal of Fracture 159(2): 219-232.

[16] K.D. DUGDALE - *Yielding of Steel Sheets Containing Slits.* J. Mech. Phys. Solids, 8, pp. 100- 104 (1960).

[17] W. ELBER (1971) - *The Significance of Fatigue Crack Closure.* ASTM STP 486: 230-242

[18] W. ELBER - *Fatigue Crack Closure under Cyclic Tension.* Engineering Fracture Mechanics. 2, pp.37-45 (1970).

[19] N.A. FLECK (1988) - *Influence of Stress State on Crack Growth Retardation.* American Society for Testing and Materials 1: 157-183.

[20] R.G. FORMAN, V.E. KEARNEY, R.M. ENGLE - *Numerical Analysis of Crack Propagation in Cyclic-Loaded Structures.* J. Basic Engng., Trans. ASME D89, pp.459-464, (1967).

[21] F. FREMY, S. POMMIER, E. GALENNE, S. COURTIN, J.C. LE-ROUX - *Load Path Effet on Fatigue Crack Propagation in I+II+III Mixed Mode Conditions - Part 2 : Finite Element Analyses.* Int Jal of Fatigue. Vol 62. Pages 113-118. 2014 DOI

[22] F. FREMY, S. POMMIER, M. PONCELET, B. RAKA, E. GALENNE, S. COURTIN, J.C. LE ROUX - *Load Path Effect on Fatigue Crack Propagation in I + II + III Mixed Mode Conditions – Part 1: Experimental Investigations*. Int Jal of Fatigue. Vol 62. Pages 104-112. 2014

[23] H. FUEHRING, T. SEEGER - *Dugdale Crack Closure Analysis of Fatigue Cracks under Constant Amplitude Loading*. Engng. Fracture Mech. 11, pp. 99-122 (1979).

[24] H. GAO, S. UPUL(1996) - *Effect of Non-Proportionnal Overloading in Fatigue Life.* Fat. Fract. Eng. Mat. Struct. 19: 1197-1206.

[25] R. GERVAIS-MOLINS - *Oxydation de superalliages à base nickel.* Thèse de l'Ecole Nationale Supérieure des Mines de Paris, 1995

[26] A. GRAVOUIL, N. MOËS, T. BELYTSCHKO (2002) - *Non-Planar 3D Crack Growth by the Extended Finite Element and Level Sets - Part II: Level Set Update.* International Journal for Numerical Methods in Engineering 53(11): 2569-2586.

[27] R. HAMAM, S. POMMIER, F. BUMBIELER - *Mode I Fatigue Crack Growth Under Biaxial Loading*. Int Jal of Fatigue. Vol 27. Num 10. Pages 1342-1346. 2005

[28] R. HAMAM, S. POMMIER, F. BUMBIELER - *Variable Amplitude Fatigue Crack Growth, Experimental Results and Modelling*. Int Jal of Fatigue. Vol 29. Num 9-11. Pages 1634-1646. 2007

[29] G. HOCHSTETTER - *Propagation des fissures à haute temperature dans le superalliage N18 pour disques de turbomachine. Interactions entre la nature des sollicitations mécaniques et des effets d'oxydation.* Thesis of ENSMP, Paris, 1994

[30] F. HOURLIER, A. PINEAU(1982) - *Propagation of Fatigue Cracks under Polymodal Fatigue.* Fatigue of Engineering Materials and Structures, Vol5 (4), pp. 287-302.

[31] J. TONG , S. DALBY , J. BYRNE , M.B. HENDERSON , M.C. HARDY - *Creep, Fatigue and Oxidation in Crack Growth in Advanced Nickel Base Superalloys.* International Journal of Fatigue 23, 897–902, 2001

[32] K. KARHUNEN - *Über Lineare Methoden in der Wahrscheinli - Chkeitsrechnung*. Mat.-Phys., 37 (1947), 1–79.

[33] S. KRUCH, J-L. CHABOCHE, S. PRIGENT - *A Fracture Mechanics Based Fatigue-Creep-Environment Crack Growth Model at High Temperatures.* Int. J. Press. Vess. And Pipping, 59:141-148, 1995

[34] J-C. LAUTRIDOU, J-Y. GUEDOU, Y. HONNORAT - *Effects of Inclusions on LCF Life of PM Superalloys for Turboengines Disks,* Conf. high temperature materials for power engineering, eds. Kluwer academics publishers, 1163, 1990

[35] V. LAZARUS, J. B. LEBLOND, ET AL. (2001) - *Crack Front Rotation and Segmentation in Mixed Mode I+III or I+II+III. Part I: Calculation of Stress Intensity Factors.* Journal of the Mechanics and Physics of Solids 49(7): 1399-1420.

[36] J. LEMAITRE, J.L. CHABOCHE(1988). *Mécanique des matériaux solides.*

[37] C. S. LI(1989) - *Vector Ctd Criterion Applied to Mixed-Mode Fatigue Crack-Growth.* Fatigue & Fracture of Engineering Materials & Structures 12(1): 59-65.

[38] P. LOPEZ-CRESPO, S. POMMIER - *Numerical Analysis of Crack Tip Plasticity and History Effects under Mixed Mode Conditions*. Journal of Solid Mechanics and Materials Engineering, Outstanding Researches by Promising Young Researchers in Mechanics and Materials Division III. Vol. 2 (2008), No. 12, pp 1567-1576

[39] A. M. A. MAGEED, R. K. PANDEY (1992) - *Studies on Cyclic Crack Path and the Mixed-Mode Crack Closure Behavior in Al-Alloy.* International Journal of Fatigue 14(1): 21-29

[40] R. C. MCCLUNG (1991) - *Crack Closure and Plastic Zone Sizes in Fatigue.* Fatigue & Fracture of Engineering Materials & Structures 14(4): 455-468.

[41] A.J. McEVILY, R. J. DONAHUE, et al. (1972) - *Crack Opening Displacement and Rate of Fatigue Crack Growth.* International Journal of Fracture Mechanics 8(2): 209-219.

[42] R. MOLINS, G. HOSCHTETTER, J-C. CHASSAIGNE, E. ANDRIEU - *Oxydation Effects on the Fatigue Crack Growth of Alloy 718 at High Temperatures.* Acta. Mater., Vol 45, N°2, pp. 663474, 1996

[43] H. NAYEB-HASHEMI, M. E. TASLIM (1987) - *Effects of the Transient Mode-II on the Steady-State Crack-Growth in Mode-I.* Engineering Fracture Mechanics 26(6): 789-807.

[44] P. NEUMANN (1969) - *Coarse Slip Model of Fatigue.* Acta Metallurgica 17(9):1219-&.

[45] P. NEUMANN (1974) - *The Geometry of Slip Processes at a Propagating Fatigue Crack—II.* Acta Metallurgica 22(9): 1167-1178.

[46] J.C. NEWMAN (1976) - *A Finite-Element Analysis of fatigue crack closure.* American Society for Testing and Materials: ASTM STP 590, pp. 281-301.

[47] J.C. NEWMAN, W. ELBER (1988) - *Mechanics of Fatigue Crack Closure.* ASTM STP 982 PA 19103.

[48] R. M. N. PELLOUX (1969) - *Mechanisms of Formation of Ductile Fatigue Striations.* Asm Transactions Quarterly 62(1): 281-&.

[49] S. PERUSIN - *Conséquences de l'oxydation haute température sur l'injection de défauts et le comportement mécanique des matériaux métalliques.* Thèse de l'Institut Polytechnique de Toulouse, 2004

[50] R. PIPPAN, J. POKLUDA (2005) - *Can Pure Mode III Fatigue Loading Contribute to Crack Propagation in Metallic Materials?* Fatigue & Fracture of Engineering Materials & Structures 28(1-2): 179-185.

[51] R. PLANK, G. KUHN (1999) - *Fatigue Crack Propagation under Non-Proportional Mixed Mode Loading.* Engineering Fracture Mechanics 62(2-3): 203-229.

[52] S. POMMIER - *Cyclic Plasticity of a Cracked Structure Submitted to Mixed Mode Loading.* Key Engineering Materials. Vol 348-349. Pages 105-108. 2007

[53] S. POMMIER, R. HAMAM - *Incremental Model for Fatigue Crack Growth Based on a Displacement Partitioning Hypothesis of Mode I Elastic-Plastic Displacement Fields.* Fatigue & Fracture of Engineering Materials & Structures. Vol 30. Num 7. Pages 582-598. 2007

[54] S. POMMIER, P. LOPEZ-CRESPO, P.Y. DECREUSE (2009) - *A Multi-Scale Approach to Condense the Cyclic Elastic-Plastic Behaviour of the Crack Tip Region into an Extended Constitutive Model.* Fatigue & Fracture of Engineering Materials & Structures 32(11): 899-915.

[55] S. POMMIER, M. RISBET - *Time-Derivative Equations for Fatigue Crack Growth in Metals*. Int Jal of Fracture. Vol 131. Num 1. Pages 79-106. 2005

[56] S. POMMIER, M. RISBET - *Time-Derivative Equations for Mode I Fatigue Crack Growth in Metals.* Int Jal of Fatigue. Vol 27. Num 10. Pages 1297-1306. 2005

[57] J. QIAN, A. FATEMI (1996) - *Mixed Mode Fatigue Crack Growth: A Literature Survey.* Engineering Fracture Mechanics 55(6): 969-990.

[58] J.R. RICE, R. THOMSON (1974) - *Ductile Versus Brittle Behavior of Crystals*. Philosophical Magazine, vol. 29, p.78.

[59] J.A. RUIZ-SABARIEGO, S. POMMIER - *Oxidation Assisted Fatigue Crack Growth under Complex Non-Isothermal Loading Conditions in a Nickel Base Superalloy*. Int. J. Fatigue, vol. 31, pp. 1724–1732, (2009)

[60] J. SCHIJVE - *An evaluation of a Fatigue Crack Growth Prediction Model for Variable Amplitude Loading* (PREFFAS), NLR – 537, (1987).
[61] J. SCHIJVE - *Some Formulas for the Crack Opening Stress Level.* Engineering Fracture Mechanics, 14, pp. 461-465 (1981).
[62] E. THIEULOT-LAURE, S. POMMIER, S. FRECHINET - *A Multiaxial Fatigue Failure Criterion Considering the Effects of the Defects.* Int Jal of Fatigue. Vol 29. Num 9-11. Pages 1996-2004. 2007
[63] E.K. TSCHEGG (1983) - *Mode-III and Mode-I Fatigue Crack-Propagation Behavior under Torsional Loading.* Journal of Materials Science 18(6): 1604-1614.
[64] A.K. VASUDEVAN, K. SADANANDA, R.L. HOLTZ - *Analysis of Vacuum Fatigue Crack Growth Results and its Implications*. International Journal of Fatigue 27 (2005) 1519–1529
[65] R.P. WEI, G.W. SIMMONS - *Recent Progress in Understanding Environment-Assisted Fatigue Crack Growth.* Int. J. Fract., 17(2), 235–247, 1981
[66] H. WESTERGAARD (1939) - *Bearing Pressures and Cracks.* Journal of Applied Mechanics, 6:49–53.
[67] O.E. WHEELER - *Spectrum Loading and Crack Growth.* ASMR 72 MetX also G.D. Report FZM 5602, (1970)
[68] J. WILLENBORG, R.M. ENGLE, H.A. WOOD - *A Crack Growth Retardation Model Using an Effective Stress Concept*. AFFDL-TM-71-1-FBR. (1971).
[69] S.T. WLODEK, M. KELLY, D. ALDEN - *The Structure of N18 Superalloys.* Ed S. D;. Antolovitch et al., T.M.S, 467-476, 1992
[70] G.A. WOODFORD - *Gas Phase Embrittlement and Time Dependent Cracking of Nickel Based Superalloys*. Energy Materials, Vol 1, No 1, pp 59-79, 2006

AUTHOR

Sylvie Pommier graduated from the Ecole Centrale de Lyon (ECL - 1992) and from the Ecole Centrale Paris (French PhD in 1995). She first joined the Ecole Centrale Paris as a faculty member (1995-2003) and then the Ecole Normale Supérieure de Cachan as a Professor in Mechanical Engineering.
From 2009 to 2012 she was the Dean of the doctoral School of the Ecole Normale Supérieure de Cachan (ENS Cachan). From 2012 to 2014 she was vice-president of ENS Cachan in charge of research and doctoral training and was involved in the set-up of the doctoral college of University Paris Saclay. Since 2014, she has been in charge of the doctoral college of University Paris Saclay.
Sylvie Pommier is a specialist in fracture mechanics and works in the field of defect tolerance design methods under non-linear conditions (inelastic material behavior, non-isothermal loading conditions, chemo-mechanical coupling, mixed-mode crack growth under non-linear conditions) for aerospace, nuclear and naval applications.